

Flavor singlet mesons in QCD

C. McNeile, C. Michael,* and K. J. Sharkey

Theoretical Physics Division, Dept. of Mathematical Sciences, University of Liverpool, Liverpool L69 3BX, United Kingdom

(UKQCD Collaboration)

(Received 3 July 2001; published 5 December 2001)

We study the flavor singlet mesons from first principles using lattice QCD. We explore the splitting between flavor singlet and nonsinglet mesons for vector and axial mesons as well as the more commonly studied cases of the scalar and pseudoscalar mesons.

DOI: 10.1103/PhysRevD.65.014508

PACS number(s): 11.15.Ha, 12.38.Gc, 14.40.Cs

I. INTRODUCTION

The splitting in mass of flavor singlet and nonsinglet mesons with the same quark content arises from gluonic interactions. The assumption that these are small is known as the Okubo-Zweig-Iizuka (OZI) rule. For the pseudoscalar mesons this splitting is not small (it is related to the η , η' mass difference), basically because of the impact of the anomaly. For scalar mesons the splitting is also expected to be large because of mixing with the nearby scalar glueball. It is usually assumed that the OZI rule is in good shape for the vector and axial mesons. This is difficult to check experimentally because of mass shifts induced by decays, etc.

Here we study this splitting from first principles using lattice QCD. We work in a simplified world with $N_f=2$ flavors of degenerate quarks. This is still sufficient to explore the sign and magnitude of any splitting which can then have a phenomenological impact on the interpretation of the observed spectrum. In this $N_f=2$ world, isospin is exact so we classify the flavor singlet state as m_0 and the non-singlet as m_1 . We indeed do find that the splitting is largest for the scalar and pseudoscalar mesons, but we are able to estimate the magnitude of the splitting for vector and axial (both f_1 , a_1 and h_1 , b_1 types of axial) mesons. For the vector and axial channels, the corresponding glueball masses are known from lattice studies [1–3] to be much heavier and so the expectation is that the splitting $m_0 - m_1$ due to such glueball effects would be small and negative (since mixed states repel). This is the same sign as found for scalar mesons but opposite to that for pseudoscalar mesons. The usual explanation for the splitting in the pseudoscalar channel is through the topological charge density in the vacuum [4,5].

In lattice studies it is possible to measure separately the non-singlet contribution which is given by the connected correlation $C(t)$ while the flavor singlet contribution has an additional disconnected correlation $D(t)$. Previous lattice studies have been made of the pseudoscalar mesons [6–10] and scalar mesons [11–14]. For a discussion including some results for vector and axial mesons, see [15].

At large t where ground state contributions dominate we have

$$C(t) = ce^{-m_1 t} \quad (1)$$

and

$$C(t) + D(t) = de^{-m_0 t} \quad (2)$$

where m_0 is the flavor singlet mass and m_1 the flavor non-singlet mass. Now if the same meson creation and destruction operators are used for the study of both correlations, with quarks degenerate in mass, d and c have the same sign.

Then by a study of D/C which is given by

$$D/C = (d/c)e^{(m_1 - m_0)t} - 1 \quad (3)$$

one can explore the mass splitting between flavor singlet and non-singlet. We illustrate this behavior in Fig. 1, assuming that only ground state contributions occur at all t values. Although it might be thought that $d=c$, we have shown previously [14] that this is not necessarily the case, and indeed sign changes in D/C versus t can be required. So, in summary, the slope (increase/decrease) of D/C on a lattice can determine the sign and magnitude of $m_1 - m_0$.

This has already been explored in detail by us for the cases of pseudoscalar mesons [10] (where $m_0 - m_1 > 0$) and

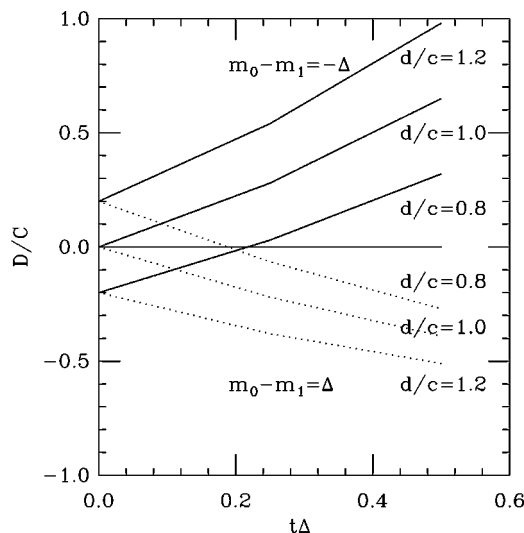


FIG. 1. The ratio of disconnected to connected contributions as given by Eq. (3).

*Electronic address: cmi@liverpool.ac.uk

TABLE I. Flavor singlet mesons produced by different operators $\bar{\psi}\Gamma\psi$ and the sign factors r_4 and r_5 as defined in the text whose product determines $D(0)/C(t)$. Here k is a spatial index and both Γ and γ are Hermitian. The meson quantum numbers are quoted in the continuum limit; for a discussion of the appropriate representation of the cubic group on a lattice see [16]. We also include our observed evidence for sign changes in $D(t)$ from $t=0$ which gives a prediction of the sign of the non-singlet minus singlet mass shift as shown.

Γ	J^{PC}	meson	r_4	r_5	$D(0)/C(t)$	$D(t)/D(0)$	$m_1 - m_0$
γ_5	0^{-+}	η, η'	-1	1	-	+	-
$i\gamma_4\gamma_5$	0^{-+}	η, η'	-1	-1	+	-	-
γ_k	1^{--}	ω, ϕ	-1	-1	+	-	-
$i\gamma_4\gamma_k$	1^{--}	ω, ϕ	-1	1	-	+	-
I	0^{++}	f_0	1	1	+	+	+
γ_4	0^{+-}	\hat{f}_0	1	-1	-	?	?
$i\gamma_5\gamma_k$	1^{++}	h_1	1	-1	-	+	-
$i\gamma_4\gamma_5\gamma_k$	1^{+-}	f_1	1	1	+	-	-

scalar mesons [14] (where $m_0 - m_1 < 0$). Here we extend the study to vector and axial mesons.

II. CONNECTED AND DISCONNECTED CONTRIBUTIONS

Here we discuss in general what information is available on the connected correlation C and disconnected correlation D . We discuss their relative sign in one gauge sample. An average over many such samples is taken in practice.

For this section we consider only local operators to create a meson, namely $\bar{\psi}_A\Gamma\psi_B$, where subscripts refer to the flavor of the quarks. We choose a basis of Hermitian matrices for Γ , see Table I. Here we restrict ourselves to spatially symmetric operators; a fuller description which takes into account also the lattice cubic symmetry is given in [16].

For $t > 1$ we can use reflection positivity to determine the sign of C . This corresponds to using a meson sink $\bar{\psi}_B\Gamma^R\psi_A$ with $\Gamma^R = \gamma_4\Gamma^\dagger\gamma_4 = r_4\Gamma$. Then the correlation

$$C(t) = (\bar{\psi}_A\Gamma\psi_B)_0(\bar{\psi}_B\Gamma^R\psi_A)_t \quad (4)$$

will be positive for $t > 1$. We evaluate this correlation in the usual way for the connected correlation, combining the Grassmannian fermion fields into propagators, which yields another minus sign, and using the γ_5 Hermiticity of the Wilson-Dirac fermion matrix to relate these propagators to a common source. We indeed find that $C(t) > 0$ in our measured correlations for $t \geq 1$.

In the flavor singlet case, when quarks $A = B$, there is an additional disconnected correlation $D(t)$ to be evaluated. This correlation can be written in the form

$$D(t) = N_f r_4 r_5 L(0) L^*(t) \quad (5)$$

where the disconnected loop

$$L(t) = \text{Tr} \Gamma M^{-1} \quad (6)$$

with M^{-1} the quark propagator and the sum in the trace is over color, Dirac and spatial indices at time t .

The factor of r_5 arises since the Wilson-Dirac fermion matrix M is γ_5 Hermitian and hence L is real/imaginary as $\gamma_5\Gamma = r_5\Gamma\gamma_5$ with $r_5 = \pm 1$. Now at $t=0$ we have that $L(0)L^*(0) > 0$ so the disconnected correlation $D(0)$ has sign $r_4 r_5$. If this sign were to be maintained at larger t , then this would give a prediction for the sign of D/C and hence information on the sign of $m_1 - m_0$ without any lattice evaluation at all. The reality is that indeed a sign change in D as t increases is possible and it is indeed the goal of this work to explore this on the lattice.

From Table I, we can deduce that there must be such sign changes in $D(t)$ as t increases from 0, since there are two operators available to study both pseudoscalar and vector mesons. In each case these two operators have different signs of $r_4 r_5$ and hence one of them must change sign so that they agree on a common value of $m_0 - m_1$ at large t where the ground state contribution must dominate. This has already been explored for the pseudoscalar case [10] and there $D(t)$ for $\Gamma = i\gamma_4\gamma_5$ was found to change sign.

III. LATTICE METHODOLOGY

Here we use dynamical fermion configurations with $N_f = 2$ from UKQCD [17]. The sea quarks correspond to $\kappa = 0.1395$ with a tadpole improved clover formalism with $C_{SW} = 1.76$.

Local and spatially-fuzzed operators [18] are used for meson creation (with two fuzzed links in a spatially symmetric orientation with 5 iterations of fuzzing with coefficient given by $2.5 * \text{Straight} + \text{Sum of staples}$). Thus we evaluate a 2×2 matrix of local and fuzzed correlators [18]. Mesons created by all independent products of gamma matrices are evaluated. Here we restrict our attention to the momentum zero sector.

We measure the disconnected correlations on 252 configurations of size $12^3 24$ separated by 20 trajectories. For the evaluation of the disconnected correlators, we use stochastic noise sources with variance reduction using the hopping parameter expansion [14]. Here we employ more noise sources (96) to explore the very small disconnected contributions from some quantum numbers. We use sources at every site on the lattice and determine the momentum zero correlations from them.

The connected correlator is obtained by explicit inversion from a source (local or fuzzed) at the origin for 126 configurations separated by 40 trajectories [17].

A. Stochastic noise compared to signal

We measure the zero momentum disconnected loop $L(t)$ on each time-slice for each gauge configuration. This ensemble, for each choice of operator Γ gives us the values of the standard deviation σ_{obs} given in Table II. We also, from our 96 stochastic samples in each case, have the estimate of the standard deviation σ_{stoch} on the mean of these 96 samples coming from the stochastic method. We can then deduce the true standard deviation of the gauge time slices from σ_{gauge}

TABLE II. Mesons produced by different operators $\bar{\psi}\Gamma\psi$. The standard deviation of the loop operator of Eq. (6) is presented. Here σ_{stoch} is the error estimated from the 96 stochastic samples, and this is used to deconvolute the observed spread to give the true standard deviation of the loop (σ_{gauge}).

Γ	J^{PC}	σ_{obs}	σ_{stoch}	σ_{gauge}
γ_5	0^{-+}	20.82	5.85	19.88
$i\gamma_4\gamma_5$	0^{-+}	9.63	4.05	8.74
γ_k	1^{--}	4.33	3.91	1.86
$i\gamma_4\gamma_k$	1^{--}	8.74	3.82	7.86
I	0^{++}	47.70	4.50	47.49
γ_4	0^{+-}	3.90	3.75	1.07
$i\gamma_5\gamma_k$	1^{++}	7.26	3.97	6.08
$i\gamma_4\gamma_5\gamma_k$	1^{+-}	13.04	3.86	12.46

$=(\sigma_{\text{obs}}^2 - \sigma_{\text{stoch}}^2)^{1/2}$. This is presented in Table II. Here the normalization is such that $M = 1 + \kappa \dots$.

In an ideal world we would have $\sigma_{\text{stoch}} \ll \sigma_{\text{gauge}}$ which would imply that no appreciable error arose from the stochastic methods employed. For the previously studied cases, the pseudoscalar with $\Gamma = \gamma_5$ and the scalar with $\Gamma = I$, we see that the stochastic errors are truly negligible with 96 stochastic samples and indeed the 24 samples used before [14,10] were adequate. For the other cases, which have been little studied hitherto, we see that the stochastic errors are reasonably small, except for $\Gamma = \gamma_k$ or γ_4 . The latter case has spin exotic quantum numbers and is expected to be very poorly determined by our methods. For the vector meson, however, one of our goals is to explore the singlet mass splitting. Here we see that more stochastic samples (over 1000) would be needed with our current method to get the stochastic error significantly smaller than the inherent gauge error. We do not have the required computational resources at present. One small advantage, however, is that we can average over the three spin components of the vector which reduces errors by $1/\sqrt{3}$. Also the second operator ($\Gamma = i\gamma_4\gamma_k$) which creates a vector meson has a relatively smaller stochastic error. We also use fuzzed sources in order to obtain more measurements.

B. Results

We present in Figs. 2–4 some of our results for the ratio of the disconnected correlator to the connected correlator. The error on the disconnected correlator is much larger than that on the connected one. This arises essentially because the absolute error on the disconnected correlator stays at the same magnitude as t increases, much as is the case for correlations between Wilson loops as used in glueball studies. The connected correlator, in contrast, has an approximately constant relative error as t increases. For this reason we employ the full data set to determine the disconnected correlator: sources at all sites and measurements every 20 trajectories. We bin these results to avoid any problem from autocorrelations among the gauge configurations separated by only 20 trajectories. Even with this approach, the error on the disconnected correlator rises rapidly as seen from the

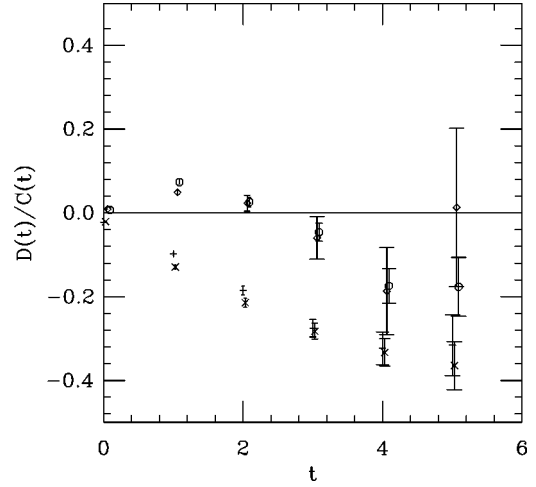


FIG. 2. The ratio of disconnected to connected contributions for pseudoscalar mesons versus time in lattice units. Local and fuzzed operators with $\Gamma = \gamma_5(+, \times)$ and with $\Gamma = i\gamma_4\gamma_5$ (diamond, octagon).

figures. A considerably larger number of gauge configurations will be needed to explore larger t values.

We are forced to consider the ratio of disconnected to connected correlator at rather low t -values because of the increasing errors on the disconnected correlator. We show in Fig. 5 the effective mass from the connected correlator for several of the cases of interest. This allows to judge the impact of excited states in this low t -range. As shown, the ground state contribution is dominant by $t \approx 3$.

Our results for the pseudoscalar case have been presented before [10] and are included here for comparison. We do indeed see a consistent slope for the two different γ matrix operators considered with a sign change for $\Gamma = i\gamma_4\gamma_5$ as discussed above. The mass difference $a(m_0 - m_1) \approx 0.1$ is positive here as expected since the η' is heavier than the non-singlet pseudoscalar mesons.

For the vector mesons, we again have two different γ matrix combinations available. We expect a sign change in

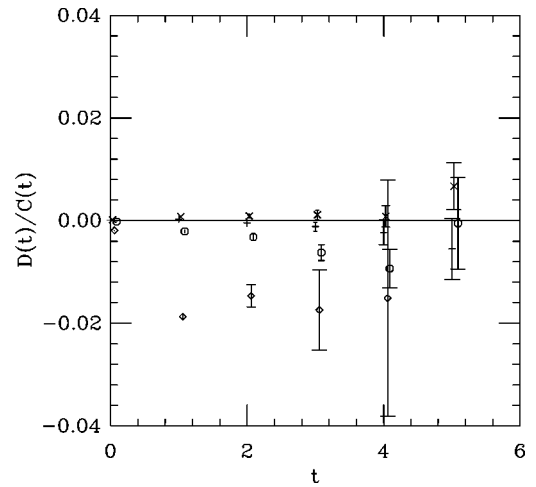


FIG. 3. The ratio of disconnected to connected contributions for vector mesons versus time in lattice units. Local and fuzzed operators with $\Gamma = \gamma_k(+, \times)$ and with $\Gamma = i\gamma_4\gamma_k$ (diamond, octagon).

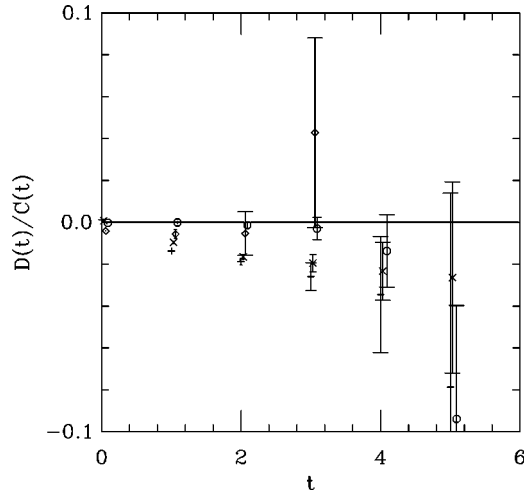


FIG. 4. The ratio of disconnected to connected contributions for axial mesons (f_1 and h_1 types) versus time in lattice units. Local and fuzzed operators for the f_1 meson with $\Gamma = i\gamma_5\gamma_k(+, \times)$ and for the h_1 meson with $\Gamma = i\gamma_4\gamma_5\gamma_k$ (diamond, octagon).

one case as discussed above. From Fig. 3 we see that the situation is that the ratio D/C is very small so that detailed study is difficult. Moreover the different values observed for fuzzed and local operators suggest that excited state contributions are significant, especially for the $\Gamma = i\gamma_4\gamma_5$ case. The results up to $t=3$ do suggest that D/C is negative and that a sign change occurs for the $\Gamma = \gamma_k$ case between $t=0$ (where it is positive) and $t=3$. This would imply $a(m_0 - m_1) > 0$.

For the axial mesons, our results are presented in Fig. 4. The f_1 meson case shows a larger signal, consistent with $a(m_0 - m_1) > 0$. We find a sign change in $D(t)$ from $t=0$ to $t>0$ for the h_1 case, giving a very small signal for $D(t)/C(t)$ at small t values which appears to be negative, implying $a(m_0 - m_1) > 0$.

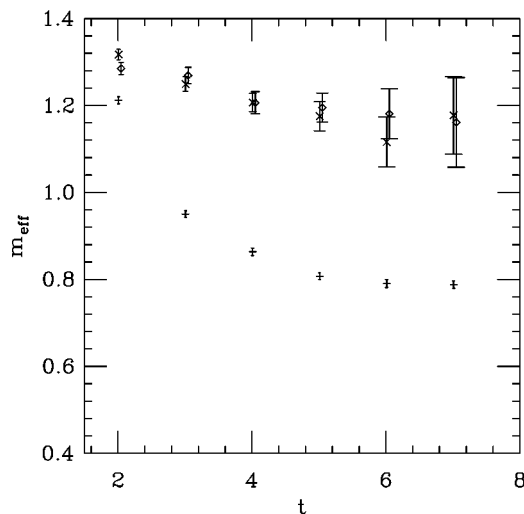


FIG. 5. The effective mass versus t (taken from correlations at t and $t-1$) for the fuzzed connected correlator for vector mesons (γ_k ; symbol $+$), 1^{++} axial mesons ($i\gamma_5\gamma_k$; symbol \times) and 1^{+-} axial mesons ($i\gamma_5\gamma_4\gamma_k$; symbol \diamond).

We have attempted to make fits to the singlet correlators to extract masses in each case, but the rapid increase in errors with increasing t makes these fits poorly determined and with results that depend strongly on the minimum and maximum t values fitted. A less sensitive way to estimate the allowed magnitude of the singlet non-singlet mass splitting is from the values of $D(t)/C(t)$ directly: bearing in mind the scenarios illustrated in Fig. 1. From the data shown for $t \leq 5$, we estimate $a(m_0 - m_1) \approx 0.10(2)$ for the pseudoscalar case, $a(m_0 - m_1) \approx 0.001(2)$ for the vector case, $a(m_0 - m_1) \approx 0.005(10)$ for the f_1, a_1 case and $a(m_0 - m_1) \approx 0.001(10)$ for the h_1, b_1 case. Note in particular the hierarchy of errors: with smallest errors for the vector case, followed by the axial mesons. Note also, as discussed above, that we have information on the sign of $a(m_0 - m_1)$ which is not folded into these error estimates.

IV. DISCUSSION

Our exploratory study has a scale set by [17] $r_0/a = 3.44$ and a pseudoscalar meson to vector meson mass ratio of $m_p/m_v = 0.71$. Using the conventional value $r_0 = 0.5$ fm then gives $a^{-1} = 1.34$ GeV while the meson mass ratio implies that the sea quarks have masses close to that of a strange quark. Here we are using $N_f = 2$ flavors of degenerate quarks in the sea. Since our lattice evaluation is for unphysical parameters, we first discuss the experimental spectrum of light quark mesons to aid in comparison with our results.

For a meson considered as made from two valence quarks of either type n (u , or d here treated as degenerate) or of type s , we have two observable non-singlet states $\bar{n}n$ and $\bar{n}s$. Then the singlet $\bar{n}n$ state would have a mass degenerate with the non-singlet $\bar{n}n$ if there were no disconnected contributions. Furthermore, from the observed non-singlet masses, by assuming an equal splitting in mass (or usually in mass squared), one also can deduce the mass which the singlet $\bar{s}s$ state would have if there were no disconnected contributions. Comparison of these theoretical mass values with the observed flavor singlet masses, then gives information from experiment about the size and nature of disconnected contributions.

Thus there are two observed states in the nonet with isospin zero which can have a component of the disconnected contribution and these can mix in terms of their quark content. So for the flavor singlet sector, we then have contributions to the mass squared matrix with quark model content $(u\bar{u} + d\bar{d})/\sqrt{2}$ and $s\bar{s}$ (which we label as nn and ss respectively):

$$\begin{pmatrix} m_{nn}^2 + 2x_{nn} & \sqrt{2}x_{ns} \\ \sqrt{2}x_{ns} & m_{ss}^2 + x_{ss} \end{pmatrix}. \quad (7)$$

Here m corresponds to the mass of the flavor non-singlet eigenstate as discussed above and is the contribution to the mass coming from connected fermion diagrams while x corresponds to the contribution from disconnected fermion diagrams. In the limit of no mixing (all $x=0$, the OZI sup-

pressed case), then we have the quenched QCD result that one flavor singlet state is degenerate with the isospin one $\bar{n}n$ meson while the other corresponds to the $s\bar{s}$ meson.

Using as input m_{nn} , m_{ss} and the flavor singlet masses m_0 and m'_0 , the three mixing parameters x cannot be fully determined. However if one makes some assumption about the mixing parameters x one can deduce the mixing pattern—see [10] for a discussion of this for pseudoscalar mesons. One simple case that may be used is to assume that all mixing strengths x are the same for mesons of a given J^{PC} . Furthermore, if the value of $x^2/(m_{ss}^2 - m_{nn}^2)$ is small, then the off-diagonal contribution to mixing is negligible and the flavor singlet mass eigenstates will be of mass squared $m_{nn}^2 + 2x$ and $m_{ss}^2 + x$. This gives two opportunities to estimate x from the observed spectrum. Also the mass shift of the nn flavor singlet ($2x$) is just the same as in the case of $N_f=2$ degenerate quarks—which is the case we explore on the lattice here. A caveat applies for axial mesons: since charge conjugation is not a good quantum number for the $\bar{s}n$ states, there will be mixing between the $J^{PC}=1^{++}$ and 1^{+-} mesons. This complicates the mixing scheme further.

We now present the conclusions of such an analysis based on the experimental [19] mass values. For the vector mesons, the $\bar{n}n$ sector gives $m_0 - m_1 = 0.013$ GeV while the $s\bar{s}$ sector gives 0.016 GeV with a mass squared formalism and 0.001 GeV with a linear mass formalism. These signs suggest that the splitting in the $N_f=2$ sector would be $m_0 - m_1 \approx 0.01$ GeV.

For the axial mesons, the additional mixing of the $\bar{n}s$ states only allows an analysis if more assumptions are made. Then assuming that the lightest iso-singlet state is predominantly $\bar{n}n$ yields the two flavor result that $m_0 - m_1 \approx 0.05, -0.06$ GeV for the $J^{PC}=1^{++}, 1^{+-}$ mesons respectively.

A complication that arises in comparing with experimental meson spectra is that of decays. In our lattice studies, since the quark mass is relatively heavy (heavier than the strange quark since $m_p/m_v=0.71$ while we expect [10] this ratio to be 0.682 for strange quarks) then we have no decay channels open for the ground state mesons we study. In contrast, some of these mesons have substantial experimental decay widths (150 MeV for the ρ , over 250 MeV for the a_1 and 140 MeV for the b_1). One consequence of this, as has been known for a very long time [20], is that the pole in the

complex plane corresponding to a resonance has an energy whose real part is lower than the quoted value which corresponds to a phase shift of 90° . This mass shift arises from the energy dependence of the width and will be more significant for wider resonances. Aside from this inherent uncertainty, there may be further dynamical effects arising from the back-reaction of the decay channels to the effective propagator.

Thus we should interpret our results as giving an indication of the strength and sign of OZI violating contributions to the light meson spectrum. These need not correspond to those observed experimentally because of the above issues (namely the more complex mixing schemes allowed for $N_f=3$ and the decay effects) and also because we would need to extrapolate our lattice results to the continuum limit and to more realistic quark masses. In particular, there is evidence from the pseudoscalar mesons that the splitting does increase with decreasing quark mass [6–10].

We find a hierarchy of singlet non-singlet mass splitting which is large for pseudoscalar mesons [0.13(2) GeV], smaller for axial mesons [0.007(13) GeV for f_1 and 0.001(13) GeV for h_1] and smallest for vector mesons [0.002(3) GeV]. This is in agreement with the hierarchy of magnitudes seen experimentally. We find that in each case the sign of the effect is that the flavor singlet state is heavier. This is the sign found experimentally for the pseudoscalar, vector and 1^{++} axial but not for the 1^{+-} axial. The magnitudes we find are smaller than the experimental values (except for the h_1 case where the magnitude is comparable), which can come in part from the use of too heavy a light quark (as is known to be the case for the pseudoscalar mesons) but also from the impact of the large experimental decay widths.

In this study we have explored from first principles in QCD the OZI rule for the meson masses for the case of two degenerate quark flavors. It would be interesting to extend this lattice study to OZI rule effects in meson decays. We find that the disconnected contributions (i.e. OZI violating terms) to the masses are indeed small for axial and vector mesons. For the vector and axial mesons, we find evidence that the flavor singlet mass is increased compared to the non-singlet. This is the opposite of what would be expected in the simplest theoretical model: namely mixing with a heavier glueball of the same J^{PC} . An understanding of this remains a theoretical challenge.

-
- [1] UKQCD Collaboration, G.S. Bali *et al.*, Phys. Lett. B **309**, 378 (1993).
 [2] C.J. Morningstar and M.J. Peardon, Phys. Rev. D **56**, 4043 (1997).
 [3] C.J. Morningstar and M.J. Peardon, Phys. Rev. D **60**, 034509 (1999).
 [4] G. 't Hooft, Phys. Rev. Lett. **37**, 8 (1976).
 [5] T. Schafer and E.V. Shuryak, Rev. Mod. Phys. **70**, 323 (1998).
 [6] Y. Kuramashi, M. Fukugita, H. Mino, M. Okawa, and A. Ukawa, Phys. Rev. Lett. **72**, 3448 (1994).
 [7] CP-PACS Collaboration, A. Ali Khan *et al.*, Nucl. Phys. B (Proc. Suppl.) **83**, 162 (2000).
 [8] W. Bardeen, A. Duncan, E. Eichten, and H. Thacker, Phys. Rev. D **62**, 114505 (2000).
 [9] SESAM Collaboration, T. Struckmann *et al.*, Phys. Rev. D **63**, 074503 (2001).
 [10] UKQCD Collaboration, C. McNeile and C. Michael, Phys. Lett. B **491**, 123 (2000).
 [11] W. Lee and D. Weingarten, Nucl. Phys. B (Proc. Suppl.) **63**, 194 (1998).

- [12] W. Lee and D. Weingarten, Nucl. Phys. B (Proc. Suppl.) **73**, 249 (1999).
- [13] W. Lee and D. Weingarten, Phys. Rev. D **61**, 014015 (2000).
- [14] UKQCD Collaboration, C. McNeile and C. Michael, Phys. Rev. D **63**, 114503 (2001).
- [15] N. Isgur and H. B. Thacker, Phys. Rev. D **64**, 094507 (2001).
- [16] UKQCD Collaboration, P. Lacock, C. Michael, P. Boyle, and P. Rowland, Phys. Rev. D **54**, 6997 (1996).
- [17] UKQCD Collaboration, C.R. Allton *et al.*, Phys. Rev. D **60**, 034507 (1999).
- [18] UKQCD Collaboration, P. Lacock, A. McKerrell, C. Michael, I.M. Stopher, and P.W. Stephenson, Phys. Rev. D **51**, 6403 (1995).
- [19] Particle Data Group, C. Caso *et al.*, Eur. Phys. J. C **3**, 1 (1998).
- [20] C. Michael, Phys. Rev. **156**, 1677 (1967).